GESEP – Gerência de Especialistas em Sistemas Elétricos de Potência

Título:

DISCRETIZATION METHODS APPLIED TO HARMONIC CURRENT DETECTION BASED ON SOGI-PLL STRUCTURES: A COMPARATIVE STUDY

Autor:

Rodrigo Cassio de Barros

Orientador:

Prof. Dr. Heverton Augusto Pereira

Membros:

Prof. Dr. Victor Flores Mendes

Prof. Ms. Allan Fagner Cupertino

Aprovação:

16 de novembro de 2017

Universidade Federal de Viçosa - UFV

Centro de Ciências Exatas e Tecnológicas - CCE

Departamento de Engenharia Elétrica - DEL

DISCRETIZATION METHODS APPLIED TO HARMONIC CURRENT DETECTION BASED ON SOGI-PLL STRUCTURES: A COMPARATIVE STUDY

Rodrigo Cassio de Barros

Orientador : Prof. Dr. Heverton Augusto Pereira

Viçosa, 16 de Novembro de 2017.

Universidade Federal de Viçosa - UFV

Centro de Ciências Exatas e Tecnológicas - CCE

Departamento de Engenharia Elétrica - DEL

DISCRETIZATION METHODS APPLIED TO HARMONIC CURRENT DETECTION BASED ON SOGI-PLL STRUCTURES: A COMPARATIVE STUDY

Rodrigo Cassio de Barros

Trabalho de Conclusão de Curso submetido ao Departamento de Engenharia Elétrica da Universidade Federal de Viçosa para a obtenção dos créditos referentes à disciplina Monografia e Seminário do curso de Engenharia Elétrica.

Orientador : Prof. Dr. Heverton Augusto Pereira

Viçosa, 17 de Novembro de 2017.

RODRIGO CASSIO DE BARROS

DISCRETIZATION METHODS APPLIED TO HARMONIC CURRENT DETECTION BASED ON SOGI-PLL STRUCTURES: A COMPARATIVE STUDY
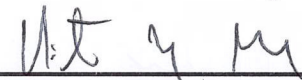
Monografia apresentada ao Departamento de Engenharia Elétrica do Centro de Ciências Exatas e Tecnológicas da Universidade Federal de Viçosa, para a obtenção dos créditos da disciplina ELT 490 – Monografia e Seminário e cumprimento do requisito parcial para obtenção do grau de Bacharel em Engenharia Elétrica.
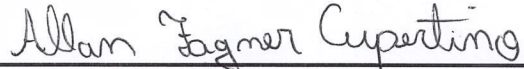
Aprovada em 16 de Novembro de 2017

COMISSÃO EXAMINADORA

_____
Prof. Dr. Heverton Augusto Pereira - Orientador
Universidade Federal de Viçosa

_____
Prof. Dr. Victor Flores Mendes - Membro
Universidade Federal de Minas Gerais

_____
Prof.M.Sc Allan Fagner Cupertino - Membro
Centro Federal de Educação Tecnológica de Minas Gerais

*À minha família e
aos meus amigos.*

"Tenho a impressão de ter sido uma criança brincando à beira-mar, divertindo-me em descobrir uma pedrinha mais lisa ou uma concha mais bonita que as outras, enquanto o imenso oceano da verdade continua misterioso diante de meus olhos."

Isaac Newton

Agradecimentos

Primeiramente, obrigado a Deus e aos meus pais, José Maria e Gurdiana, pelo suporte incondicional. Obrigado por ensinarem que humildade e dedicação são as maiores armas que posso ter. Aos meus irmãos Tiago, Thais e Cândido por sempre me apoiarem e conceder o calor do amor fraternal. Aos meus cunhados, Ana Claudia e Wesley, por serem tão atenciosos e presentes. A minha sobrinha e afilhada Helena, por trazer tanta luz. Aos meus avós, tios(as) e primos(as), em especial ao Tarlley, pela parceria e conselhos. A todos os amigos de engenharia, república, intercambio e aos demais que contribuíram para essa conquista. Aos professores pelos ensinamentos, em especial ao Prof.Heverton. Obrigado ao GESEP, pelo amadurecimento e experiência.

Sumário

Resumo

A operação multifuncional de inversores fotovoltaicos (PV) consiste em fornecer serviços auxiliares à rede elétrica, tais como: injeção de potência reativa, compensação de corrente harmônica e regulação de frequência. Tais serviços são realizados quando os inversores estão trabalhando abaixo da condição nominal. Assim, a operação multifuncional pode melhorar a qualidade de energia da rede. Quando o inversor fotovoltaico é usado para compensação de corrente harmônica, ele funciona como filtro ativo. Existem vários métodos de detecção de corrente harmônica, e a estrutura de detecção deve ser simples, precisa e rápida. Neste trabalho é proposta uma melhoria no método de detecção de harmônicos baseado no *Generalized Integrator Phase Locked Loop* (SOGI-PLL). Esta estrutura detecta os componentes de corrente harmônicas predominantes. Quando o processo de discretização é aplicado ao SOGI-PLL, alguns erros podem afetar a velocidade e a precisão. A melhoria do método de detecção é realizada inserindo uma retroalimentação negativa na estrutura SOGI. Na primeira parte deste trabalho, os modelos matemáticos e as simulações são realizados usando cinco combinações de métodos de discretização, sendo eles: *Forward Euler*, *Backward Euler*, *Tustin* e *Tustin com Prewarping*. Serão discutidos os resultados de detecção de cada método bem como o desempenho da retroalimetação negativa. Primeiramente será feita uma análise de como estes métodos de discretização afetam o diagram de Bode da função de transferência do estágio que detecta o conteúdo harmônico. O detector também será analisado separadamente escolhendo combinações estratégicas de ordens harmônicas e frequências de amostragem. Por fim, o detectopr é usado em um inversor fotovoltaico multifuncional e a compensação de componentes harmônicas é discutida.

Abstract

The multifunctional operation of photovoltaic (PV) inverters consists in provide ancillary services to the power grid, such as: reactive power injection, harmonic current compensation and frequency regulation. Thus, the multifunctional operation can improve the ac-grid power quality. When the PV inverter excess capacity is used to harmonic current compensation, it works as active filter. There are several harmonic current detection methods, and the detection structure should be simple, accurate and fast. In this work is proposed an improvement in the harmonic detection method based on the Second Order Generalized Integrator coupled with a Phase Locked Loop (SOGI-PLL). This structure detects the most predominant harmonic current components. When the discretization process is applied to the SOGI-PLL, some errors can degrade the speed and accuracy. The improvement of the detection method is realized inserting a negative feedback path in the SOGI structure. In the first part, the mathematical model and simulations are performed using five combinations of discretization methods. The methods discussed in this work are: Forward Euler, Backward Euler, Tustin and Tustin with Prewarping. First, an analysis of how these discretization methods affect the Bode diagram of harmonic transfers function is made. The detector is also analyzed separately, choosing strategic combinations of harmonic orders and sampling frequency. Finally, the detector is used in a multifunctional photovoltaic inverter. In all cases, the results of harmonic components detected and the negative feedback performance is analyzed.

List of Tables

List of Figures

Chapter 1

Introduction

In the last decade, photovoltaic (PV) power systems have experienced fast growth around the world (REN21, 2017). Predictions show that solar energy will grow by 20 % per year until 2020 and solar power prices are rapidly falling to the point where solar became cheaper than on-shore wind power (Schmela and Masson, 2016). According to Global Market Outlook for Solar Power, the market of PV power will keep growing, as shown in Figure 1.1 Moreover, PV power systems already contribute to a good share of electrical power in many countries, such as Italy, Germany and Greece. However, the growth of renewable energy, especially photovoltaic sources, makes the grid more decentralized and susceptible to disturbances (de Andrade et al, 2016). This fact is bringing some concerns to professionals in these areas and one of the most discussed points is the grid power quality, due to use of power electronic based-converters.

Although the benefits of PV systems are many, there is a excess capacity in the PV inverter, since the system does not work at all during nighttime and does not work on full capacity during low profile irradiance (de Andrade et al, 2016). Due to this fact, multifunctional inverters are being studied to work on ancillary tasks, resulting in a better usage of the installed PV power system and improving the quality of the power running through the grid (Varma et al, 2011).

Since solar irradiance varies during the day, PV inverters usually work below its nominal operation point (de Andrade et al, 2016), as illustrated in Figure 1.2. Thus, whenever inverter power does not exceed nominal value, it can be used to improve the power quality. Ancillary services such as reactive power compensation (Akagi et al, 1984), reactive injection during faults, voltage and frequency regulation and harmonic current compensation (Pereira et al, 2015b) are some of the contributions that PV inverters can

aggregate to improve the power quality of the electrical grid.
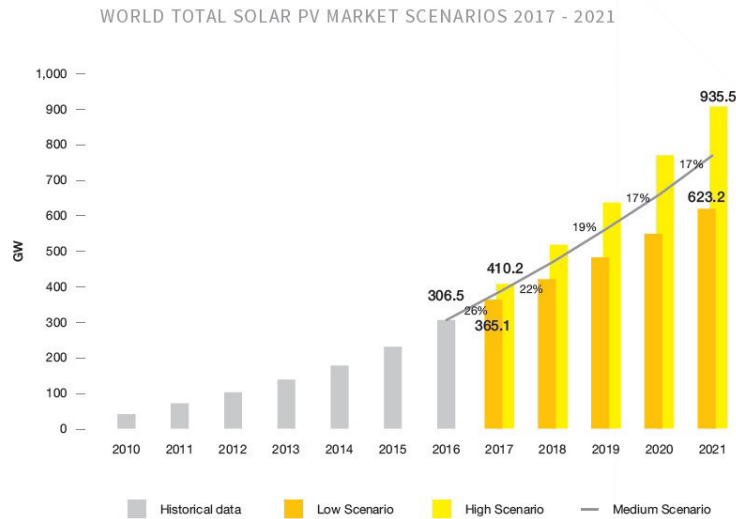
Figure 1.1: World Total Solar PV Market Scenarios 2017 - 2021 (Global Market,2017)
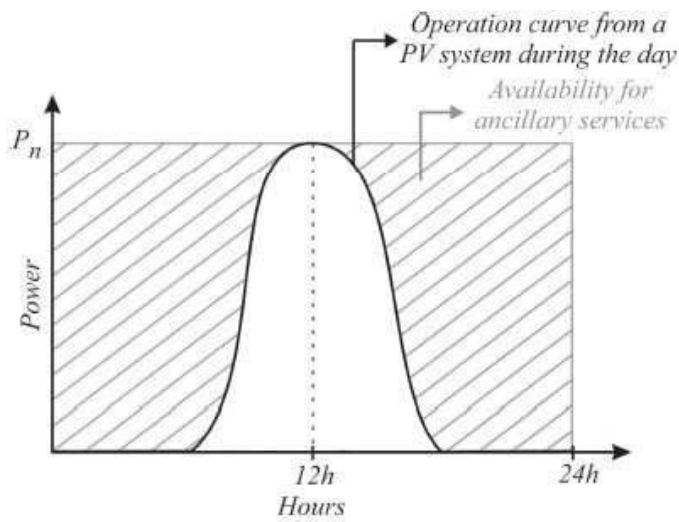
Figure 1.2: Operation Curve from a PVC System during the Day (Guilherme L. E. da Mata,2016)

In order to use the PV inverter working with harmonic compensation, a precise structure of harmonic detection needs to be provided. Also, because

of the complexity and sensibility of this detector structure, choosing the best discretization method is very relevant. This fact can decrease error in the detection stage and improve the compensation process. Thus, the multifunctional inverter will provide better results in grid power quality.

1.1 Objectives

Because of the increasing of the nonlinear loads connected into the grid, the current harmonic distortion is something which had been worrying professionals in the area. Traditional solution uses active and passive filters to reduce the harmonic distortion. The second solution is to use photovoltaic multifunctional inverter in order to improve grid power quality doing harmonic current compensation. This operation happens when the PV inverter is working below the nominal conditions. SOGI-PLL structures can be used to detect multiple harmonic components. However, harmonic detector used in this process is considered a complex structure which needs to be very fast and accurate. Therefore, when the discretization process is applied, the methods needs to be well chosen. The performance of the methods and their implementation complexity needs to be taken in account. Therefore, this work has a goal to make a comparative study of the discretization methods during the harmonic current compensation.

1.2 Text Organization

This work is divided in seven chapters. The second chapter is composed by a brief Literature review about the topics which are important to understand the proposals of this work. The third chapter presents the methodology, which is divided in the harmonic detector structure with the mathematical equations and the discretization methods. Chapter 4 , 5 and 6 are designated to show the methods performances in different conditions of tests. Finally, in chapter 7 is presented the conclusions, considering a comparative analysis. Also, the future proposes are presented.

Literature Review

2.1 Harmonic Distortion

The increased use of solid state devices at the consumer end has introduced a power quality issue. The nonlinear load brings current harmonic distortion. The magnitude of this harmonic distortion varies with the nonlinear nature (Abbas and Saqib, 2007). Harmonic current can be generated due to nonlinear loads such as computers, printers, rectifiers and fluorescent lamps.

High levels of harmonic distortion can cause undesirable effects such as increased transformer, capacitor, motor or generator heating, effect the performance of electronic equipment (which relies on voltage zero crossing detection or is sensitive to wave shape), incorrect readings on power metering, interference with telephone circuits, etc (Macii et al, 2017).

2.2 Active and Passive Filters

Traditionally, passive power filter are used as a solution for harmonic distortion, caused by the system harmonics, since they are easy to design, having simple structure, low cost and high efficiency (Peterson et al, 2008). However, they have some issues related to their controllers. Traditionally, there are several drawbacks, which provides only fixed compensation, generates resonance problem and are bulky in size.

In order to improve this point, active filter are constantly used to compensate the harmonic distortion presented in the grid current (Pinto et al,

2007). Those filters are introduced to compensate the current harmonics and reduce the total harmonic distortion. Even active filters have great performance, they are relativity expensive, and they need a considerable physical space. For photovoltaic power system, those filters can be replaced by the PV inverter which is able to compensate harmonics components when they are not completely used to inject active power to the grid. This fact can save space and cost caused by the active filter.

2.3   Harmonic Current Detection and Compensation

In order to use the PV inverter for harmonic current compensation, an important issue, which needs to be defined, is the harmonic current detection method. Different strategies have been proposed in the literature. References (Bonaldo et al, 2016), (Pereira et al, 2015b), apply the conservative power theory for current decomposition in three orthogonal components, the active, void and residual current component. In (Akagi et al, 1984), it is used the instantaneous power theory to separate the current in average and oscillating components. Reference (Tummuru et al, 2014) uses the instantaneous symmetrical components theory for extracting the reference currents. It should be emphasized that the detected harmonic current by the traditional methods contains all harmonic orders, and it increases the controller tuning complexity. Therefore, additional computational processing is necessary to identify individual harmonic currents (Tummuru et al, 2014).

In three-phase applications with harmonic compensation, many works use proportional-resonant (PR) controllers, due to the presence of many frequencies in the inverter current reference (He et al, 2014). In these conditions, the conventional proportional-integral (PI) controller has steady state error due to its limited current tracking capability (He et al, 2014). On the other hand, a PR controller must be tuned for each harmonic frequency in order to compensate the harmonic currents, increasing the control algorithm complexity.

The harmonic detection method proposed for single-phase PV systems in (Xavier et al, 2015) is based on two stages of second order generalized inte-

grator structure with synchronous reference frame phase-locked loop (SOGI-PLL) (Ciobotaru et al, 2006a). This method performs the detection of the predominant harmonic component in the load current. Furthermore, the frequency, phase angle and amplitude of this harmonic component are also estimated and, if the proportional-resonant controller (PR) is used, its resonant frequency can be tuned dynamically by the harmonic detector, becoming it an adaptive controller. This strategy can be interesting in terms of control complexity, once the compensation of the predominant harmonic present in the load current can be enough to regard the standards that determine the maximum index of harmonic distortion at PCC (Ciobotaru et al, 2006a).

In other cases, if more harmonic components need to be compensated, more stages can be included in the harmonic detection strategy proposed in (Ciobotaru et al, 2006a). However, add more stages in this strategy can lead to steady state error in the harmonic component detection due to non ideal filter characteristic of the SOGI-PLL structure.

2.4   Discretization Methods

Discretization is the process that transforms the continuous or numerical attribute into the categorical or nominal data (Yepes et al, 2012). Many of the existing discretization techniques cause a displacement of the poles. This fact results in a deviation of the frequency at which the infinite gain occurs with respect to the expected resonant frequency (Lavangnananda and Chattanachot, 2017). This error becomes more significant as the sampling time decrease or the desired peak frequency increase. Therefore, each method has a specific performance and the methods need to be well selected depending on the application.

The discretization methods has particular characteristic based on stability, implementation level, and dynamics control performance (Lavangnananda and Chattanachot, 2017). Forward method is easy to implement but it can transport a stable plant to an instable one (Song et al, 2014). Backward method does not have this problem of instability but it has limitation over the dynamic performance of the control system (Ciobotaru et al, 2006b). Tustin methods have great performance thinking about dynamic

behavior and stability. However, Tustin has a more sophisticated mathematical implementation and presents frequency error when the system has a resonant frequency (Song et al, 2014). In order to solve this error frequency, the Tustin with Prewarping has better performance in theory comparing to Tustin methods (Rodriguez et al, 2008).

2.5   Multifunctional Inverters: Harmonic Compensation

According to Global Market Outlook for Solar Power, the market of PV power will keep growing, being expected 935.5 GW PV market in 2021. However, with the progress of the renewable energy, including the photovoltaic sources, the concern about the grid power quality grows too, mainly due to the use of power electronic based-converters (Domingos et al, 2015). The prospects indicate that the focus will be on establishing new electricity market designs, integration of storage technologies, improving distribution and transmission lines.

Although the benefits of PV systems are many, they are seen as not entirely exploited. Since solar irradiance varies during the day, inverters usually work below its nominal operation point (Pereira et al, 2015b), as illustrated in Figure 1.2. Thus, whenever inverter power does not exceed its nominal value, and can be used to improve the power quality (Bonaldo et al, 2013). Ancillary services such as reactive power compensation (Pereira et al, 2015b), reactive injection during faults (Pereira et al, 2015b), voltage and frequency regulation (Sangwongwanich et al, 2016) and harmonic current compensation are some of the contributions that PV inverters can aggregate to improve the power system stability and power quality.

Harmonics pollution in electrical networks cause voltage distortion, additional losses and heating in the electrical equipment, perturbing torque, vibrations and noise in motors, malfunction and failures of sensitive equipment, resonances and interference with electronic equipment. Current total harmonic distortion (THD) level is an important index in power systems harmonic analysis. Some standards establish that current THD level must be below 5% (Tao et al, 2016). To reduce the grid harmonic current distortions

there are some methods found in literature. The most conventional ones use passive filters (Fujita and Akagi, 1991) and active filters or associations of both to decrease the THD level.

Methodology

3.1 Current Harmonic Detection

Dual Second Order Generalized Integrator (SOGI-PLL) structure is the harmonic detector used in this work (Rodriguez et al, 2011). The SOGI structure is an adaptive filter with characteristics of a low pass filter combined with bandpass filter. The block diagram is presented in Figure 3.1. The harmonic detection is a cascade association of a SOGI and a synchronous reference frame phase-locked loop (SRF-PLL) structure.

The tuning of the proposed structure is frequency dependency, thus problems can occur when the grid frequency has fluctuations. As a consequence an adaptive tuning of the structure is required. Therefore, the resonance frequency value of the SOGI is adjusted by the provided frequency of the PLL structure (Rodriguez et al, 2011).

The association of n structures in series can detect n harmonic components. The first stage detects the fundamental component of the load current i1 (t). After passing through this first stage, the signal consists only of the harmonic components. The following stage estimates the first harmonic current according to the largest amplitude. For example, the Stage 2 detects the largest harmonic presented in the current. If there is the Stage 3, it would identify the second largest and so on until the last stage (Stage X). In this work,two stages are performed. The negative feedback method is the return of part of an output signal to the input. A negative feedback of the estimated signals is employed, in order to improve the performance of the harmonic detector.

The transfer function of the SOGI for first stage (Fundamental component detection) in Fig.3.1, is given by:
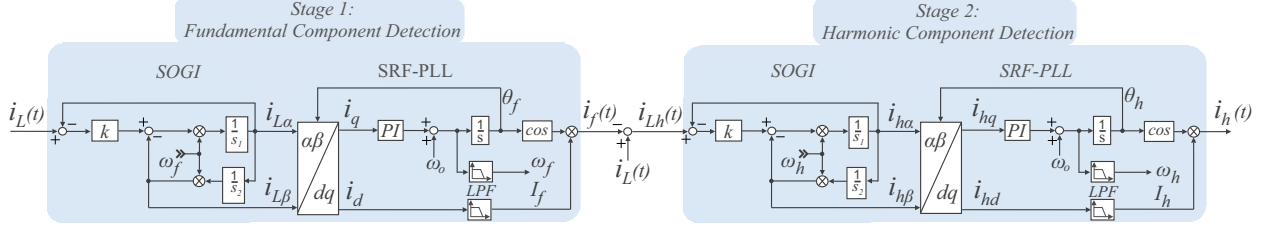
Figure 3.1: Current Harmonic Detector Based on SOGI-PLL Structure.

$$H_1(s) = G_f(s) = \frac{k\omega_f s_2}{s_1 s_2 + k\omega_f s_2 + \omega_f^2} \tag{3.1}$$

Also, the transfer function of the SOGI for second stage (Harmonic component detection) in Fig.3.1, is given by:

$$H_2(s) = G_h(s) = \frac{k\omega_h s_2}{s_1 s_2 + k\omega_h s_2 + \omega_h^2} \tag{3.2}$$

where ω_f and ω_H are the SOGI operating frequency for the fundamental and harmonic component respectively. Also, k is the damping factor Ciobotaru et al (2006a).The damping factor is responsible for the bandpass range.

3.2   Negative Feedback

The negative feedback is technique applied to have better performance during the harmonic detection process. Considering only two stages and disregarding the SRF-PLL dynamics, the block diagram is simplified as shown in Fig.3.2. G_f is the SOGI transfer function for the fundamental component detector and G_2 is the SOGI transfer function for the harmonic component.

Using the block diagram of Figure 3.2, the following transfer functions are obtained:

$$\frac{I_f(s)}{I_L(s)} = \frac{G_f(s) - G_f(s).G_h(s)}{1 - G_f(s).G_h(s)} \tag{3.3}$$

$$\frac{I_H(s)}{I_L(s)} = \frac{G_h(s) - G_f(s).G_h(s)}{1 - G_f(s).G_h(s)} \qquad (3.4)$$

which represents the frequency behavior of the proposed harmonic detector. The negative feedback introduces an anti-resonance frequency, which attenuates the frequencies different from the detected.
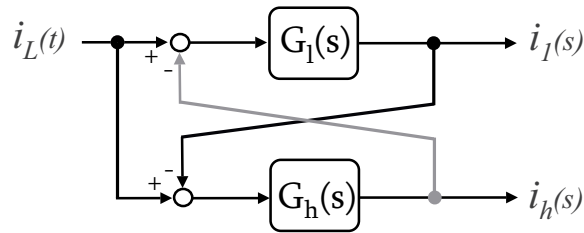
Figure 3.2: Negative Feedback Representation

3.3   Bode Diagram of the Harmonic Transfer Function

In the chapter 4 is discussed how the different discretization methods can affect the Bode diagram performance of the Harmonic Transfer Function. In addition, these analysis are made considering the detector with and without negative feedback. In order to have a better understand about the methodology used in this work, the Bode plots of the harmonic function is presented in Fig.**??**. The bode plot is plotted in the continuous dominion for two cases: with and without negative feedback in the instructor detector.

As can be noticed, $i_h(s)$ presents two important characteristics in the Bode plot: The zero gain at the harmonic frequency and the resonant peak at the fundamental frequencies. The resonant peak can generate error of frequency shift. However, this error in almost neglected for low harmonic orders. Thus, the focus in this work will be on the second point: the zero gain at the harmonic frequency.

This zero gain can be demonstrated in the continuous domain applying the limit in the harmonic transfer function. Thus, $s_1 = s_2 = s$ and they tend
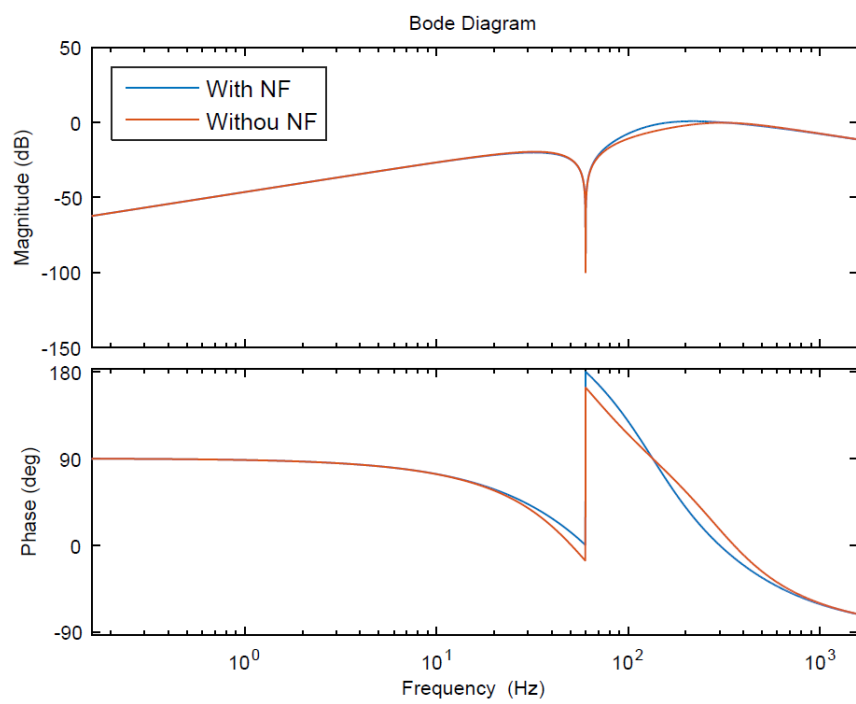
Figure 3.3: Inverter Control Strategy.

to be equal to $\omega_j h$. This equation is demonstrated as follow:

$$\lim_{s \to j\omega_h} \frac{G_f(s) - G_f(s).G_h(s)}{1 - G_f(s).G_h(s)} \tag{3.5}$$

In fact, the $\lim_{(s) \to j\omega_h} G_h(s)$ is equal to 1, because :

$$\lim_{s \to j\omega_h} G_h(s) = \lim_{(s) \to j\omega_h} \frac{k\omega_h s}{s^2 + k\omega_h s + \omega_h^2} = \frac{jk\omega_h^2}{-\omega_h^2 + jk\omega_h^2 + \omega_h^2} = 1 \tag{3.6}$$

In addition, $\lim_{(s) \to j\omega_H} G_1(s)$ is equal to generic value A, as follow:

$$\lim_{s \to j\omega_h} G_f(s) = \lim_{(s) \to j\omega_f} \frac{k\omega_h s}{s^2 + k\omega_f s + \omega_1^2} = \frac{jk\omega_f \omega_h}{-\omega_h^2 + jk\omega_f \omega_h + \omega_f^2} = A \tag{3.7}$$

Therefore:

$$\lim_{s \to j\omega_h} \frac{G_f(s) - G_f(s).G_h(s)}{1 - G_f(s).G_h(s)} = \frac{A - A.1}{1 - A.1} = \frac{0}{1 - A} = 0 \tag{3.8}$$

The unitary gain at the harmonic frequency is equal to 0 dB in the continuous operation. However, depending of the discretization methods, this fact can not be observed the discrete transfer function. Then, the discretization process can bring some errors and affect the harmonic amplitude detection. Then, the methodology used compares the magnitude value presented at the harmonic frequency.

3.4 Discretization Methods

Most of current controllers are implemented in digital platforms and it requires discrete functions. Thus, the influence of the discretization process should not be ignored once it has errors associated to its conversion (Pereira et al, 2015a). There are several discrete-time implementations of these con-

trollers. According to (Pereira et al, 2015a), because of the narrow band of the harmonic current detector, they present some sensitivity to the discretization process. Thus, it is very important to evaluate the effectiveness of the discretization alternatives, providing an accurate resonant frequency. Table I shows some discretization methods.

Table 3.1: s to z Transformation

Discretization Method	Equivalence
Forward Euler	$s = \frac{1-z^{-1}}{z^{-1}T_s}$
Backward Euler	$s = \frac{1-z^{-1}}{T_s}$
Tustin	$s = \frac{2(1-z^{-1})}{T_s(1+z^{-1})}$
Tustin with Prewarping	$s = \frac{\omega(1-z^{-1})}{tg(\frac{\omega T_s}{2})(1+z^{-1})}$

As shown in Fig. 3.1, the SOGI structure has two discretization stage represented as 1/s1 and 1/s2. Thus, two methods of Table I are combined to make the following configuration:

Table 3.2: Combinations Methods

Method 1 ($1/s_1$)	Method 2 ($1/s_2$)	Symbol
Forward Euler	Foward Euler	FF
Forward Euler	Backward Euler	FB
Backward Euler	Backward Euler	BB
Tustin	Tustin	TT
Tustin with Prewarping	Tustin with Prewarping	TP

3.5 Harmonic Current Detector Applied to Photovoltaic Multifunctional Inverter

In conventional operation, inverters are responsible to extract the maximum power from the photovoltaic array and inject it into the grid with unitary power factor ,(Romero-Cadaval et al, 2013). As can be seen in Figure 3.4, in a single phase PV system, the dc/dc stage with a boost converter is used to keep the desired dc-link voltage constant. The boost control strategy is described in (Xavier et al, 2017). Also, a LCL filter is connected after

the inverter in order to attenuate the harmonics components caused by the
PWM operation (Xavier et al, 2017). The LCL filter output and dc-link
voltage are connected to the inverter control structure.

The inverter control strategy is shown in Figure 3.5 In the dc-link voltage
control, it is used a PI compensator. The compensator calculates the active
current amplitude which is injected into the power system. This signal is
synchronized with the PCC voltage, and it is added to the signal from the
Harmonic Detector structure (Xavier et al, 2017).

The control strategy is responsible to control dc and ac simultaneously
in order to inject the maximum active power at the grid. With the harmonic
detector, the PV inverter is able to work with harmonic current compensation
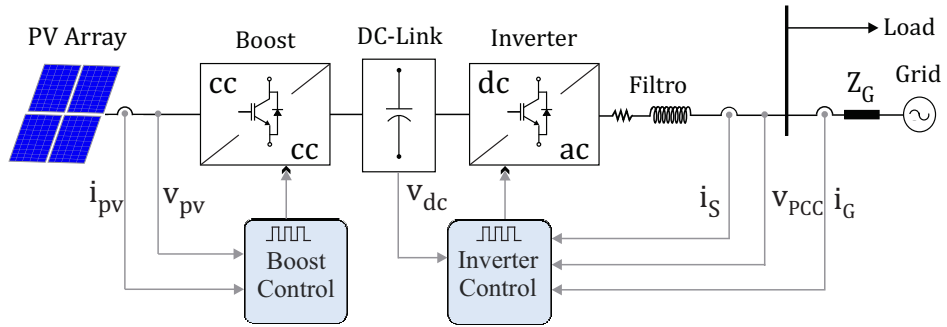when the inverter is working below the nominal operation, Xavier et al (2017).

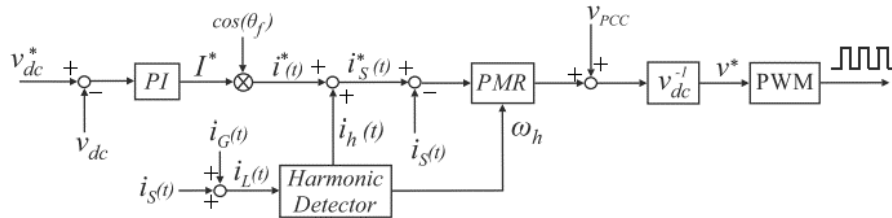Figure 3.4: Single-Phase Grid-Connected Photovoltaic System.

Figure 3.5: Inverter Control Strategy.

Results 1
Bode Diagram Analysis

As discussed in the chapter 3, the magnitude value of $H_2(S)$ should be equal to 1 pu at the harmonic frequencies. However, depending of the discretization method used, this value can have errors. In addition, this error can be modified depending of the harmonic order and sampling frequency.

In order to verify how those factors affect the harmonic component detection, the amplitude and the harmonic frequencies detected are analyzed. Therefore, the sampling frequency is varied from 5 kHz to 15 kHz and the harmonic order was varied from 2nd to 19th. Thus, the main focus was to find the magnitude value at the harmonic frequency for each discretization methods in different combinations of sampling frequency and harmonic order. In addition, the same analysis are made for two cases: with and without negative feedback at the harmonic structure detector.

The values of the magnitude found are presented in the Figure 4.1. The first important point to be focused is the discrepant results found for FF and BB, if compared to the other methods. As can be noticed, for low value of sampling frequency and high harmonic orders, the magnitude value is around 4 pu to FF and 0.6 pu to the FB. Those results, as showed in equation 3.8, was supposed to be 1 pu. Thus, the error in magnitude is almost 3 pu for FF and 0.4 pu for BB. Another point is how much the magnitude value changes when the negative feedback is used in the harmonic detector structure.As can be noticed, FF has presented improvements for harmonics components closer to the fundamental component. However, this fact is not observed to BB method. Thus, negative feedback does not make considerable changes at the results.

The FB and TT methods present similar results when the negative feed-

back is applied. As can be noticed in Figure 4.1(e)-(g), they have considerable improvements at the results for low harmonic orders, closer to 60 Hz. When the negative feedback is not applied, Figure 4.1 (f)-(h)there is an increasing of magnitude error for low harmonic orders (close to the fundamental component) in both discretization methods. In addtion, for high harmonic orders, the negative feedback does not have relevant modifications results.

Also, when the harmonic order is increased, the error also increases (considering constant the sampling frequency). Other important factor which affects directly the amplitude detection is the sampling frequency. When this value is decreased, the error in magnitude increases. This behavior is observed even for both TT and FB methods. Also, as can be noticed in Figure 4.1 (e)-(g) and 4.1 (f)-(h), there is a critical region for those two methods for high harmonic orders and low sampling frequency (even with and without the negative feedback strategy).

In addition, using negative feedback, TT presents smaller amplitude error than FB over the critical region. However, for low sampling frequencies and low harmonic order it is possible to check a better performance of the FB over the TT. Even with some different points, these two methods have great results for low harmonics order and high sampling frequencies (when the negative feedback is used).

Finally, the TP is analyzed and presents the best result between the discretization methods. Due to the capacity of tracking the harmonic frequency, this method presents great performance even for low sampling frequency and high harmonic order. Therefore, TP does not present the critical region, as FB and TT. Also, it is important to verify how the negative feedback improves the harmonic detection performance. Without negative feedback, for low harmonics order, close to the fundamental, the error in magnitude increases. However, using negative feedback, the value of the magnitude detected is almost 1 pu for all the combinations of sampling frequencies and harmonics orders.
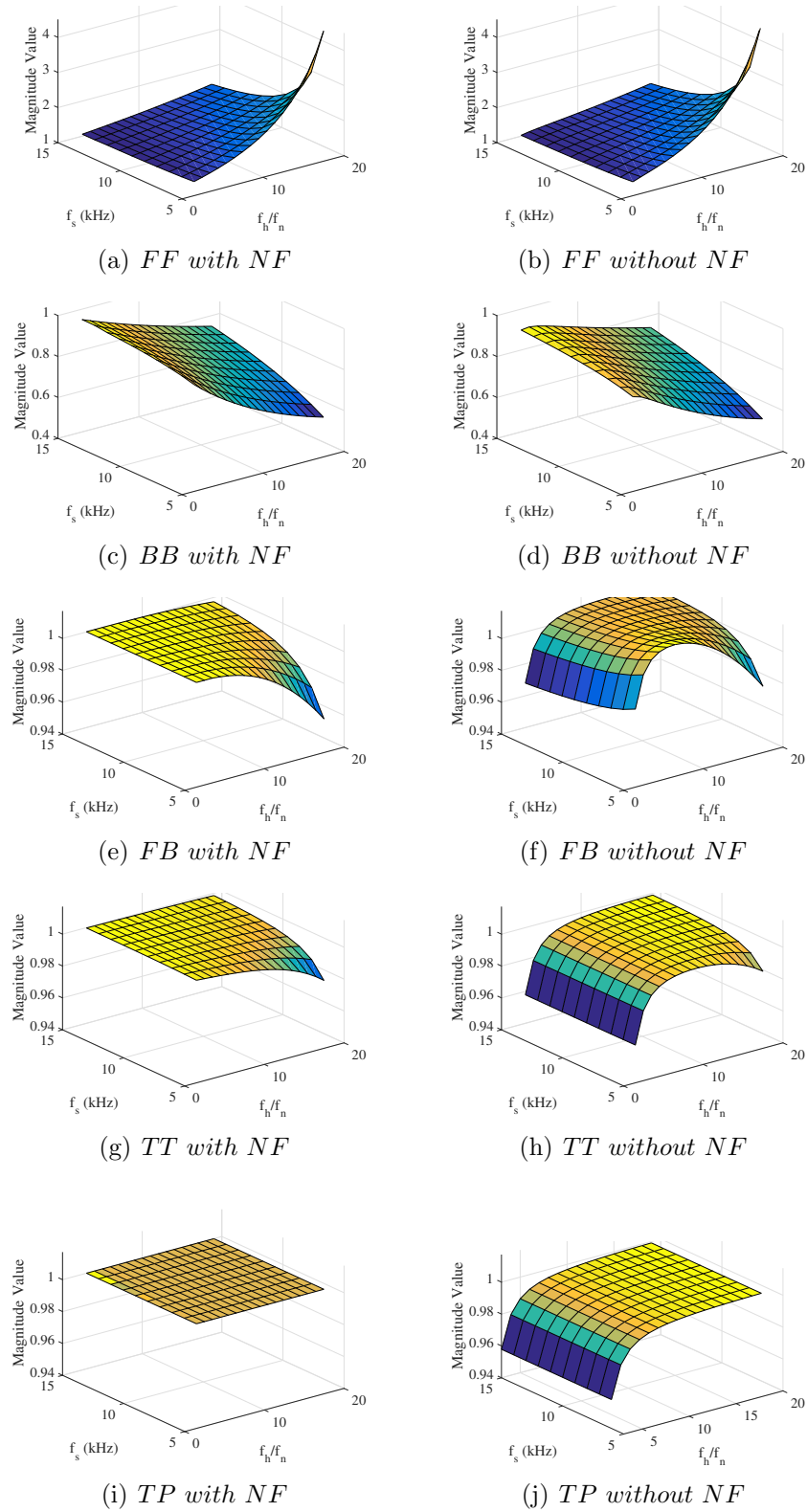
Figure 4.1: Magnitude Value detected for each discretization method in different combinations of Sampling Frequency and Harmonic Order: (*a*) *FF* with *NF* , (*b*) *FF* without *NF*, (*c*) *BB* with *NF* , (*d*) *BB* without *NF* , (*e*) *FB* with *NF*, (*f*) *FB* without *NF*, (*g*) *TT* with *NF* , (*h*)*TT* without *NF*, (*i*) *TP* with *NF*, (*j*) *TP*without *NF*

Results 2
Analysis of the Harmonic Detector Performance

In this chapter, the harmonic structure detector performance is analyzed. Some tests of specifics values of sampling frequencies and harmonic order were performed. In addition, for all the cases, the structure with and without negative feedback are discussed. Also, three testes are performed in order to validate the results mentioned in chapter 4.

5.1 Test 1: Sampling Frequency and the Harmonic Orders Impact

In the test 1, the sampling frequency and the harmonic order are varied in four different cases. They are:

Case I: In this test, all the combinations methods are simulated in low condition of sampling frequency detecting harmonics of low orders. In other words, the sample frequency is considerable with high value, equal to 15 kHz, and low harmonic orders are chosen. In the first 3 seconds of simulation, the 2nd harmonic order is injected by the nonlinear load. After this time, the harmonic component is replaced by the 7th order.

Case II: In this test, the sampling frequency is maintained equal to 15 kHz. However, high harmonic orders are chosen. In the first 3 seconds of simulation, the 15th harmonic order is injected by the nonlinear load. After this time, the harmonic component is replaced by the 19th order.

Case III: For the third case, the sampling frequency is decreased to a low value of 5 kHz. Also, low harmonic orders are chosen. In the first 3 seconds

of simulation, the 2nd harmonic order is injected by nonlinear load. After this time, the harmonic is replaced to the 7th order.

Case IV: In the last case, a critical region is analyzed. In order words, the low sampling frequency, equal to 5 kHz, is chosen and high harmonics orders are applied. In the first 3 seconds, a 15th harmonic order is applied by the nonlinear load. After this time, the harmonic component is replaced by the 19th order.

In all cases, the harmonics injected by the nonlinear load and the sampling frequency adopted in case I, II, III and IV are summarized in Table 5.1. Also, a fundamental component equal to 20 A is applied in the input of the harmonic detector as well. Thus, this component is detected by the first stage of the structure.The harmonics injected to the nonlinear load have 5 Amperes of amplitude. In order to focus in the harmonic detection process, the analysis of the results will be in the second stage. Then, the focus is on the harmonic transfer function. Therefore, the amplitude and frequency of the harmonic detected will be discussed in each case.

Table 5.1: Cases Conditions for Test 1

Cases	Harmonic Orders	Sampling Frequency	Harmonic Amplitude
Case I	2nd and 7th	15 kHz	5 A
Case II	15th and 19th	15 kHz	5 A
Case III	2nd and 7th	5 kHz	5 A
Case IV	15th and 19th	5 kHz	5 A

5.1.1 Case I: High Harmonic Frequency and Low Harmonic Orders

For case I, the amplitude and frequency of the harmonic detected using the sampling frequency of 15 kHz are showed in Figure 5.1. In Table 5.2 is presented the errors in amplitude detected for all the methods analyzed. The results are discussed in two important points: when the negative feedback is not applied and when it is applied.

- Considering the harmonic detector structure without negative feedback

to the lower harmonic (2nd), the error is equal to 1.28% for all the three cases discussed. However, for the 7th harmonic component, the error in amplitude is equal to 0.32 % in the worth case, to the *TT*. Also, *FB* presents 0.03 % of error, followed by TP with 0.08%.

- When the negative feedback is applied, the error in amplitude detected to the 2nd harmonic is reduced to 0.02 % and this value is constant for all the three methods. In addition, when the 7th is detected, the error is also reduced to *TT* and *TP* compared to the structure without negative feedback. *TP* and *FB* present 0.04 % of error and the *TT* error is reduced to 0.26%.

- Thus, without negative feedback, *TT*, *FB* and *TP* increase the error when the harmonic order is closest to the fundamental component. However, using the negative feedback, this problem is solved and *FB*, *TT* and *TP* method present smaller errors.
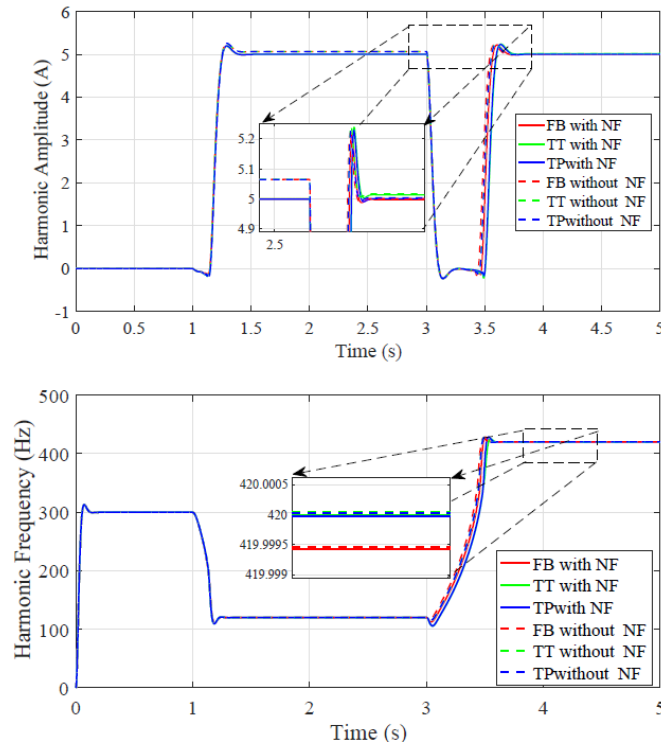

Figure 5.1: Amplitude and Frequency of the Harmonic Detected in Case I

As can be noticed in Fig.5.1, the frequency of the harmonic detected is very similar, 120 Hz the (2nd) and 420 Hz to the (7th). The difference are very small and they can be disregarded in this case. In order words, even with different discretization methods, considering or not the negative feedback, the different of frequency detected is very small.

Table 5.2: Amplitude Error, Case I

Discretization Method	Amplitude Error to (15th)	Amplitude Error to (19th)
FB with NF	0.02 %	0.04 %
TT with NF	0.02 %	0.26 %
TP with NF	0.02 %	0.04 %
FB without NF	1.28 %	0.03 %
TT without NF	1.28 %	0.32 %
TP without NF	1.28 %	0.08 %

5.1.2   Case II: High Harmonic orders and High Sampling Frequency

In case II, the results for high harmonic orders, 15th and 19th, with the sampling frequency equal to 15 kHz are showed in Figure 5.2. The errors in amplitude for all the methods are showed in Table 5.3. Thus, some points are observed:

- Considering the structure without negative feedback for the 15th harmonic component, TT is the methods which presents the largest error, equal to 1.18%. TP had the best performance, equal to 0.01 % , followed by FB, with error equal to 0.42 %. Similar behavior is observed to the 19th harmonic order. The worth case was also using TT, with an error equal to 1.84 % and the best one was using TP, with error smaller than 0.00 % , followed by FB with 0.82 %.

- In the other hand, it is possible to notice the amplitude error reduction when the negative feedback is applied to the 15th harmonic order.

However, considering the 19th harmonic component, the negative feedback does not make any improvements at the results for this case. This fact can be explained because this harmonic order is not close to the fundamental component.

• Also, it is important to see the increasing of the amplitude error with the increasing of harmonic order to *TT* and *FB*, using or not the negative feedback. In the other hand, *TP* has a lowest and constant error even in for high harmonic order.

As can be noticed in Figure 5.2, the frequency of the harmonic detected is very similar, 900 Hz the 15th and 1140 Hz to the 19th. The difference is very small and can be disregarded in this case. In order words, even with different discretization methods considering or not the negative feedback, the different of frequency detected is very small.
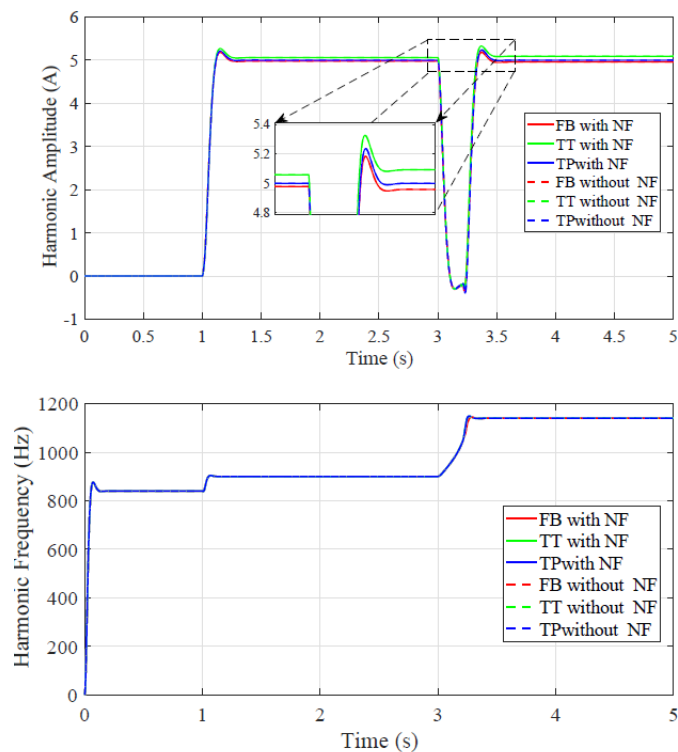

Figure 5.2: Amplitude and Frequency of the Harmonic Detected in Case II

Table 5.3: Amplitude Error, Case II

Discretization Method	Amplitude Error to 15th	Amplitude Error to 19th
FB with NF	0.42 %	0.82 %
TT with NF	1.16 %	1.84 %
TP with NF	0.00 %	0.00 %
FB without NF	0.44 %	0.82 %
TT without NF	1.18 %	1.84 %
TP without NF	0.01 %	0.00 %

5.1.3   Case III: Low Sampling Frequency and low Harmonic Orders

In case III, the same harmonics orders of case I are applied. However, the sapling frequency is decreased to 5 kHz. The amplitudes and phases of the harmonics detected are presented in Figure 5.3 and the amplitude error are showed in Table 5.3. Thus, some important points are presented:

- Comparing to case I (15 kHz), the errors increased for all the the methods when the sampling frequency is reduced to 5 kHz, using or not the negative feedback. Thus, when the sampling frequency is reduced, the error increases for all the conditions.

- Differently than case I, the 2th and 7th harmonics orders has different errors when the negative feedback is used. TP is the methods which present the best performance, flowed by FB and TT. Also, there are improvements at the results for all the methods when the negative feedback is applied. However, this fact is more expressive to the 2th harmonic because it is closer to the fundamental frequency.

- Excepting TP, all the methods are influenced by sampling frequency even using or not the negative feedback. TP is the method which has smaller error. Also, TT is the method which suffers more with the reduction of sampling frequencies for those conditions of test.

As can be noticed in Figure 5.3, the frequency of the harmonic detected is very similar, 120 Hz the (2th) and 420 Hz to the (7th). The difference are

very small and they can be disregarded in this case. Therefore, even with different discretization methods, considering or not the negative feedback, the different of frequency detected is very small.

Figure 5.3: Amplitude and Frequency of the Harmonic Detected in Case III

Table 5.4: Amplitude Error, Case III

Discretization Method	Amplitude Error to 2nd	Amplitude Error to 7th
FB with NF	0.09 %	0.84 %
TT with NF	0.1 %	1.86 %
TP with NF	0.06 %	0.06 %
FB without NF	1.34 %	0.8 %
TT without NF	1.46 %	1.92 %
TP without NF	1.30 %	0.07 %

5.1.4   Case IV: Low Sampling Frequency and High Harmonics Orders

Finally, the critical region is analyzed in case IV. The same harmonics orders showed in case II is discussed in this test. However, the sampling frequency is reduced to 5 kHz. The results are showed in Figure 5.4. The amplitude errors are showed in Table 5.5. The results are discussed as follow:

- The error in amplitude does not change when the negative feedback is applied for all the three methods and for both harmonics orders. This fact is because the harmonics frequencies are not close to the fundamental component and the sampling frequency is very low.

- The error increases when the harmonic orders increases as well, excepting for *TP*. Because of the frequency tracking used to implement this method, it is able to have a great performance at the amplitude detection, even for high harmonics orders.

- As can be noticed, the error increases when the sampling frequency decreases. This fact can be noticed when the results for case IV is compared to case II. Excepting the *TP* method, *TT* and *FB* had a considerable increasing in the amplitude error when the sampling frequency is decreased.

- In addition, the errors increases to *TT* and *FB* when the harmonic order increases as well. In other words, when the harmonic order is changed from 15th to 19th, the error increases for all the methods.

As can be noticed in Figure 5.5, the frequency of the harmonic detected is very similar, 900 Hz the 15th and 1140 Hz to the 19th. The difference is very small and can be disregarded in this case. Therefore, even with different discretization methods considering or not the negative feedback, the different of frequency detected is very small.
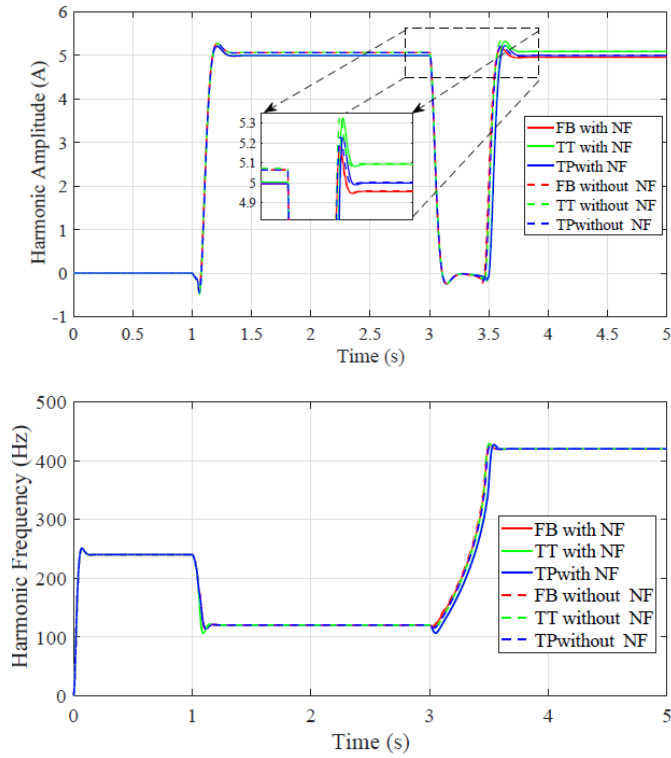
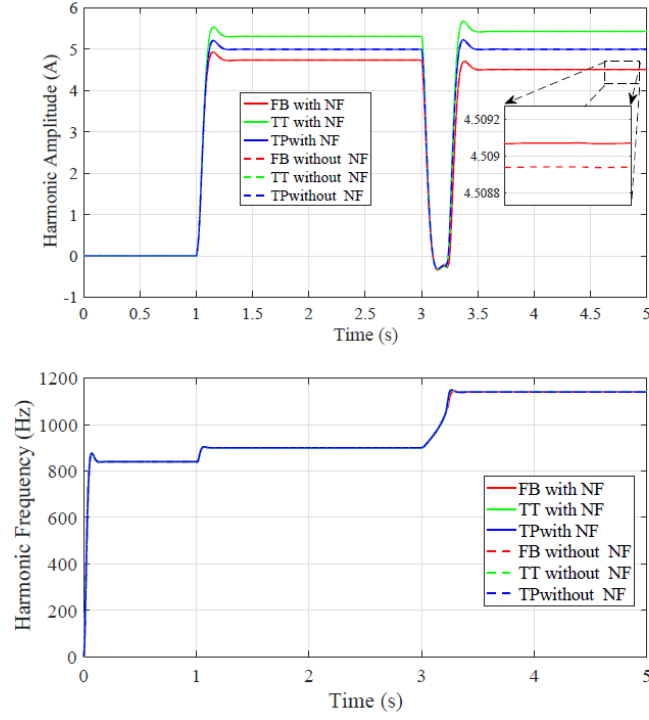Figure 5.4: Amplitude and Frequency of the Harmonic Detected in Case IV

Table 5.5: Amplitude Error, Case IV

Discretization Method	Amplitude Error to 15th	Amplitude Error to 19th
FB with NF	5.30 %	9.82 %
TT with NF	6.26 %	8.58 %
TP with NF	0.02 %	0.00 %
FB without NF	5.30 %	9.82 %
TT without NF	6.26 %	8.58 %
TP without NF	0.02 %	0.00 %

5.2   Test 2: Constant Sampling Frequency

In this test, the basic idea is to check the performance of the methods when the sampling frequency is kept constant and the harmonic order is increased. Also, this analysis are made for the harmonic detector with and without negative feedback. For this test, the sampling frequency was maintained in 12 kHz and the harmonic orders applied were 3rd, 7th, 9th and 21th. Also, each method is analyzed separately and the FB performance is shown in Figure 5.5.

As can be noticed, the error in amplitude increases with the increasing of the harmonic orders. The highest harmonic component, 21th, presents the highest error, equal to 2 %. On the order hand, the lowest one, 3rd present the lowest error. Also, it is important noticed the negative feedback effect. For high harmonics values, the negative feedback does not make considerable changes at the result, but for low orders, the negative feedback has improved the detection process. For FB method, in these conditions especially, the error with negative feedback is higher than without negative feedback.
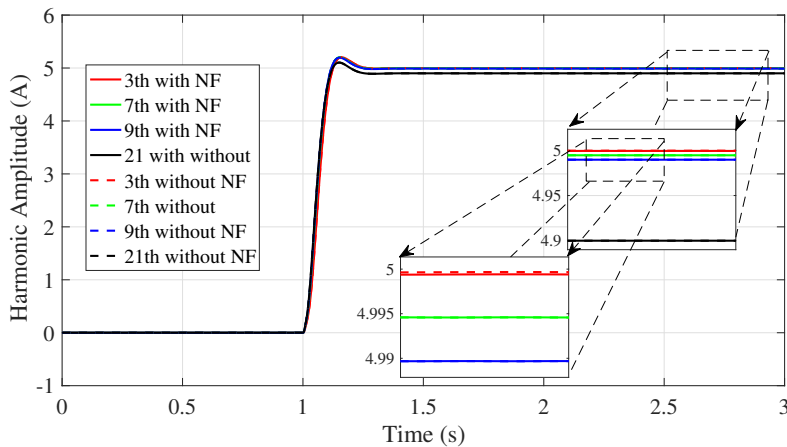

Figure 5.5: Harmonic Amplitude Detected for FB in Test 2

The same behavior was observed to the TT method. However, the error for high harmonics orders is more considerable than FB. For the highest one, 21th, the error is 3.38 %. When the harmonic order decreases, the error in amplitude detected also decreases. In addition, as observed in FB,

the negative feedback only affects the amplitude detection of low harmonic orders. Another interesting point is the detection of amplitude above 5 A in *TT*. For *FB* the amplitude detect is below 5A.

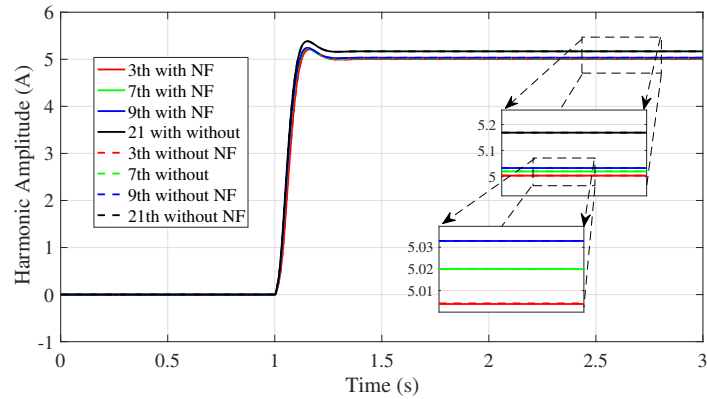Figure 5.6: Harmonic Amplitude Detected for *TT* in Test 2

Finally, the results to the *TP* methods are presented in Fig 5.7 As can be noticed, the method has a great performance when the harmonic orders are increased. Comparing to the *TT* and *FB*, *TP* is the only one which is able to detect the harmonic amplitude with minimum error for high harmonic orders.
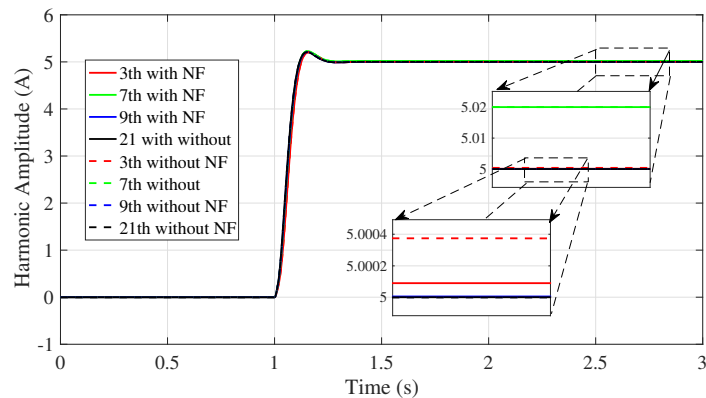

Figure 5.7: Harmonic Amplitude Detected for *TP* in Test 2

5.3   Test 3: Constant Harmonic Order

In test 03, the harmonic order is kept constant, equal to 19th, and the sampling frequency values are changed form $7\ kHz$, $12\ kHz$ and $20\ kHz$. The amplitude error was analyzed for the three tests. Also, the harmonic detector with and without negative feedback were also performed. The FB results are showed in Figure 5.8. As can be noticed, the amplitude error increases when the sampling frequency decreases. For the lowest sampling frequency, the error is around 4.46 %. Also, to the highest sampling frequency, equal to 15 kHz, the error is around 0.06 %. Thus, when the harmonic order detected is very high, 19th, the effect of the negative feedback is irrelevant.

Figure 5.8: Harmonic Amplitude Detected for FB in Test 3

The results for TT are presented in Figure 5.9 . The error also increases when the sampling frequency decreases. For the lowest sampling frequency, $7\ KHz$, the error is equal to 8.82 % and to the highest one, equal to 15 KHz, the error is reduced to 1.92 %. Again, because of the harmonic order detected is very high, 19th, the effect of the negative feedback is irrelevant.

Figure 5.9: Harmonic Amplitude Detected TT in Test 3

TP performance is presented in Figure 5.10. This method presents the best performance when the sampling frequency is varied. As can be noticed, even for low sampling frequency, the amplitude of the harmonic detected is close to 5 A. Thus, when the harmonic order detected is very high, 19th, the affect of the negative feedback is irrelevant.
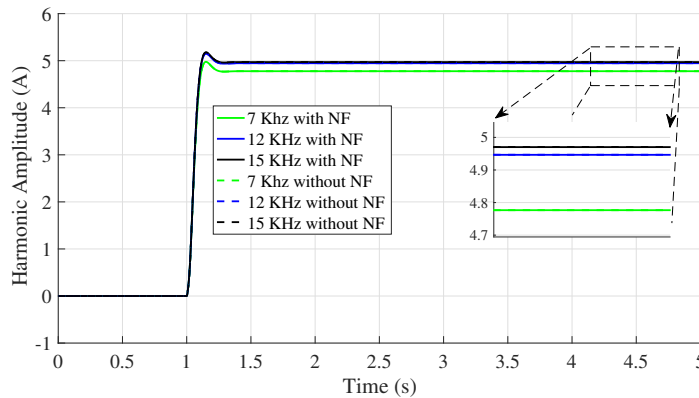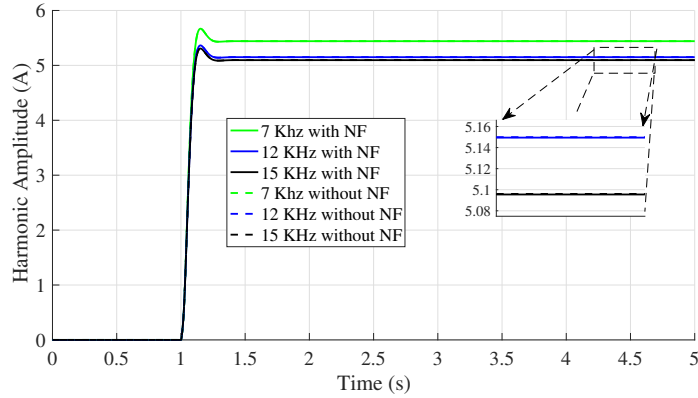

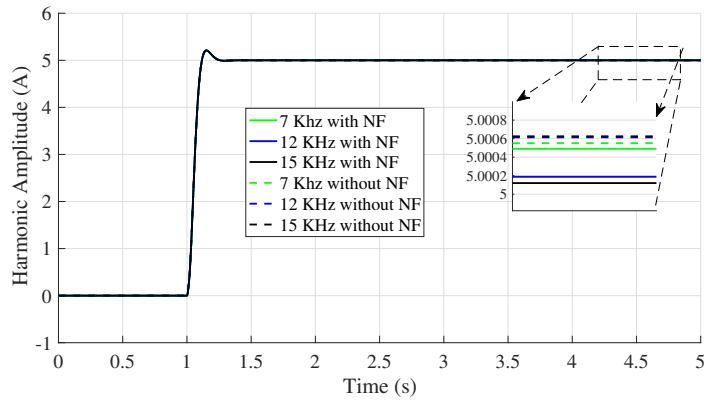Figure 5.10: Harmonic Amplitude Detected TP in Test 3

Results 3
Multifunctional Inverter: Case Study

In chapter 6, the harmonic detector is applied to a single phase PV system. The idea is to use the structure showed in the previous chapters in order to detect the harmonic components caused by the presence of nonlinear loads at the residence or industry. Once the amplitude and phase of the harmonic is detect, the inverter will create the same harmonics with opposite value in amplitude. Then, the harmonic compensation process is made and the power grid quality is improved.

In order to verify the performance of the structure detector proposed, the system will be simulated on PLECSs environment. In this simulation, the sampling frequency was considered the same value of the switching frequency. In Table 6.1, the PV panel specification are showed. Also, the simulations parameters and the controllers gains used are showed in Table 6.2 and Table 6.3.

Table 6.1: PV Panel Specification

Parameters	Value
Nominal Power	250 W
Short Circuit Nominal Current	8.5 A
Open Circuit Nominal Voltage	35.5 V
Maximum Power Point Current	7.99 A
Maximum Power Point Voltage	31.29 V

The results are separated in three cases. The idea is to analyze the influence of the harmonic order and the sampling frequency at the harmonic detection operation. In case I, a 3rd harmonic component of 5A is injected by the nonlinear load, and the sampling frequency of the detector is of 6

Table 6.2: Simulations Parameters

Description	Value
LCL filter inductors	$1\ 0\ mH/19mH\ mH$
LCL filter capacitor	$3.8\ \mu F$
LCL Filter Damping Resistance	$4\ \Omega$
PCC Voltage	$220\ V$
DC Link Voltage	$390\ V$
DC Bus Capacitor	$500\ \mu F$

Table 6.3: Inverter Control Parameters

Controllers Gains	Value
dc-link controller	$\mathrm{kp}_{sdc} = 0.145, ki_{sdc} = 1.244$
Dc/dc boot converter controllers	$\mathrm{kp}_{VM} = 1.508, ki_{VM} = 158.33$
Resonant Controller	$\mathrm{kp}_{res} = 14.833, ki_{res} = 2000$

kHz. In case II, the harmonic order is kept the same, 3rd, and the sampling frequency is increased to 12 kHz. Finally, in case III, 5 A of harmonic order , 9th, was injected with the sampling frequency equal to 12 kHz. Table 6.4 summarizes the tests conditions. The time simulation for each case was 2.2 seconds. Also, the harmonic detection begins at time of 0.8 seconds and the harmonic compensation at 0.9 seconds.

Table 6.4: Tests Conditions of Results 3

Cases	Harmonic Orders	Sampling Frequency	Amplitude Value
Case 1	3rd	$6kHz$	5 A
Case 2	3rd	$12kHz$	5 A
Case 3	9th	$12kHz$	5 A

6.1 Case I: Low Harmonic Orders and Low Sampling Frequency

The results of the amplitude detection is showed in Figure 6.1. As can be noticed, the results are improved when the negative feedback is applied to

TT and *TP*. Also, *TP* is the method with the best performance in this case, followed by *TT* and *FB*. Also, the harmonic frequency detection is presented. All the three methods have a similar performance. Then, the phase detected does not have considerable effect with the discretization methods.

As can be noticed, there are overshoot in the amplitude at the beginning of the harmonic detection. The reason for that is the time of the stabilization control of the system.
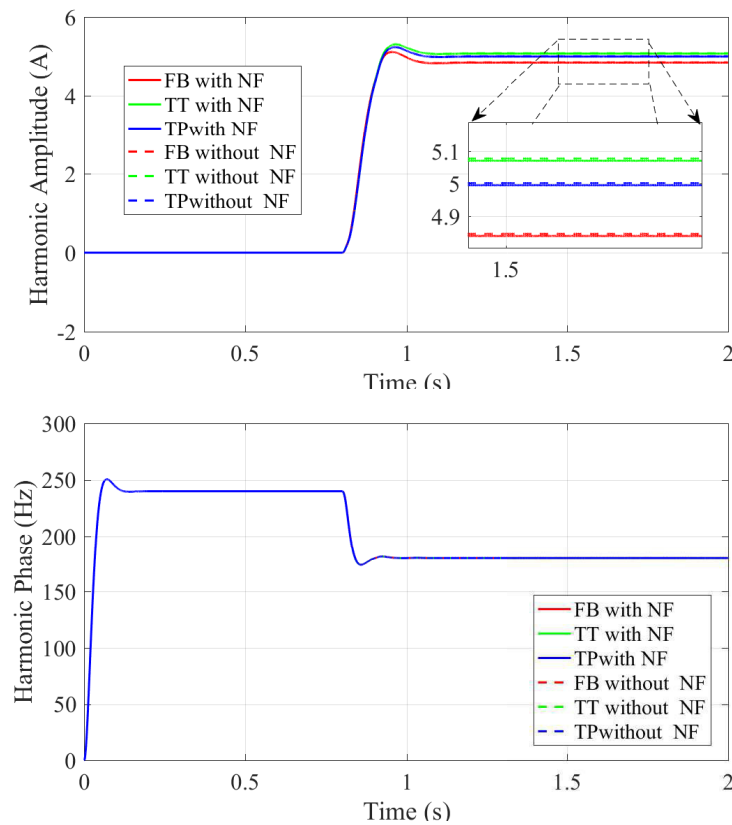

Figure 6.1: Amplitude and Frequency of the Harmonic Detected in Case I

6.2   Case II: Low Harmonic Orders and high Sampling Frequency

In case II, the harmonic injected by the nonlinear load is the same than case I. However, the sampling frequency is increased to 12 kHz. The results are showed in Figure 6.2. As can be notice, the same comportment in case I is repeated in case II. However, the error decreases for all the cases when the sampling frequency is increased to 12 kHz.

In addition, in this case, it is clear the improvement of the detection when the negative feedback is applied. Also, as can be seen, the harmonic frequency detected are very similar for all the cases.
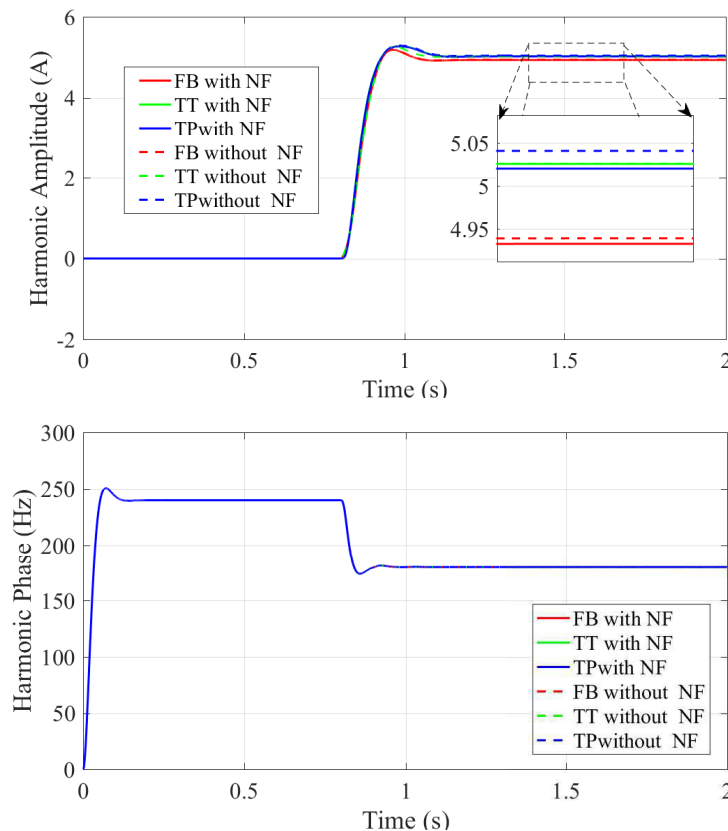

Figure 6.2: Amplitude and Frequency of the Harmonic Detected in Case II

6.3 Case III: High Harmonic Orders and high Sampling Frequency

In this case, the sample frequency is kept in 12 kHz and the harmonic order was increased to 9th. The results for the amplitude detected is showed in Figure 6.3. As can be noticed, the negative feedback does not affect a lot the amplitude of the harmonic detected. This fact can be explained because the harmonic order is not very close to the fundamental component. Also, in this case FB presents the largest error and TP is the one with the lowest error in amplitude.

Again, the frequency of the harmonic detected is showed. All the methods have similar performance, very similar.
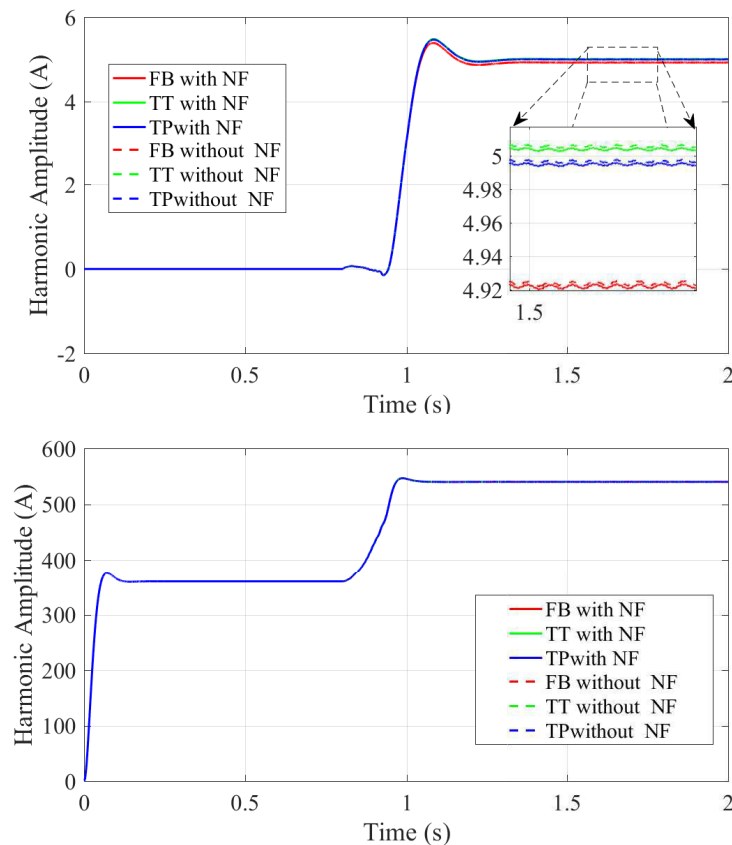

Figure 6.3: Amplitude and Frequency of the Harmonic Detected in Case III

6.4   Harmonic Compensation Process

In order to illustrate how the harmonic compensation is made, the spectrum of grid current and the PV inverter are showed in Figure 6.4 and Figure 6.5, respectively. The parameters simulations are the same presented in case II. In other words, the frequency sampling used is equal to 12kHz. The spectrum is separated in two stages: before and after the harmonic compensation.

Before the harmonic compensation, the grid presented a 3^{rd}harmonic component of 5 A and the PV inverter was not detecting any harmonic component. However, after the harmonic compensation, the PV inverter presents the 3rd component in the current spectrum. With this information, the inverter add the same amplitude of harmonic detected, with the opposite signal, to the grid current. Thus, the grid reduce the distortion, as showed in Figure 6.4. Therefore, the grid current presents improvements at the power quality after the harmonic current compensation.
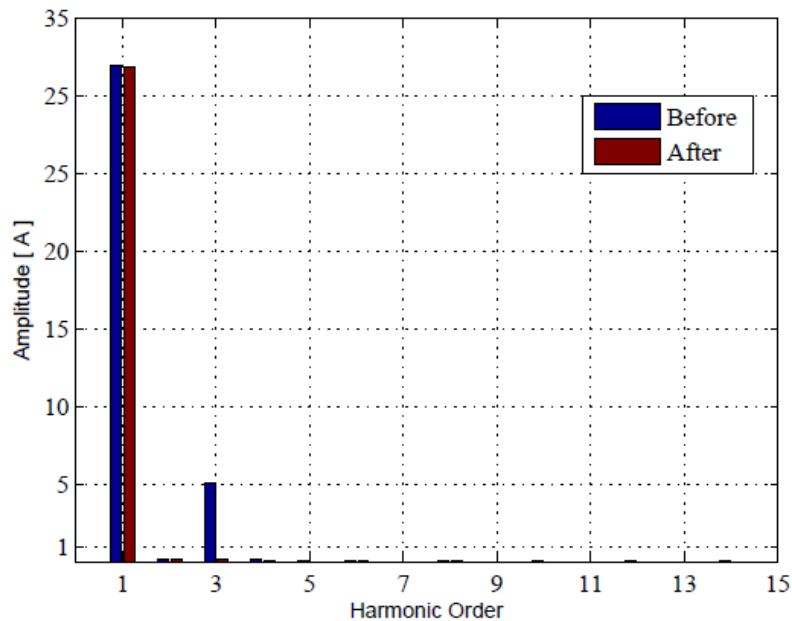

Figure 6.4: Grid Current Spectrum During the Harmonic Compensation Process
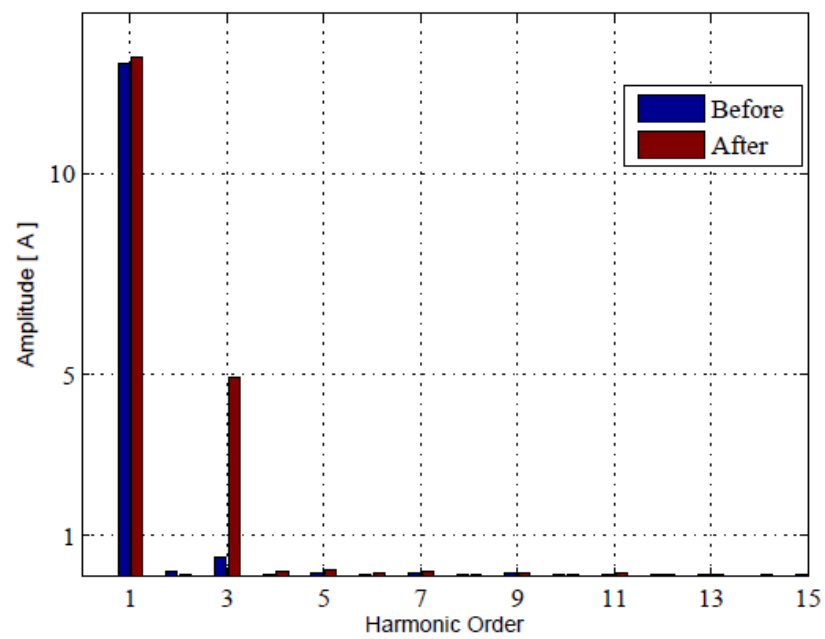
Figure 6.5: PV Inverter Current Spectrumum During the Harmonic Compensation
            Process

Chapter 7

Conclusion and Future Work

In this work is made a comparative study of different discretization methods during the harmonic current detection. The harmonic detector studied is based on the SOGI-PLL composed by two or more stages. Because of the sensitivity of the plant, the best discretization method is necessary in order to have better results at the harmonic detection. Also, the harmonic detection was performed considering a system with and without negative feedback.

It can be concluded the inefficiency of *FF* and *BB* comparing to the other methods. They presented high error to detect harmonic magnitude value. Also, for those two methods, the negative feedback do not improve considerable the results. Therefore, those two methods are not ideal to multifunctional application.

Also, can be concluded two important factors related to the amplitude error: The sampling frequency and harmonic order. For all the methods, with and without negative feedback, the error increases when the sampling frequency decreases. In addition, considering the harmonic order effect, it is possible to see the increasing of the error for harmonics orders close to the fundamental component (60 Hz) when the negative feedback is not applied. This fact happens for all the three methods discussed. However, when the negative feedback is applied, this problem is solved. In other words, using the negative feedback strategy, the harmonic detection process have considerable improvements for low harmonics frequencies in all the three discretization methods.

Therefore, the negative feedback has improved the harmonic detection for low harmonic order, for all the three cases. However, when the harmonic order are not close to the fundamental component, the negative feedback does not affect the results.

The frequency detected for all the methods were also analyzed. And the values found were very similar. Therefore, this point was not deeply discussed in this work.

FB and and *TT* have more stable results and some different characteristics. The first one presents better performance for low harmonic orders and the second one has better results for high harmonic order values. Also, both methods, even using negative feedback, presented larger error at the critical region. This critical region correspond the combination of high harmonic order and low sampling frequencies. Therefore, their applications are limited in this region.

However, *TP* is the method which presents the best results. Because of the frequency tracking in its structure, the error in amplitude are very slow and constant for all the combinations of sampling frequencies and harmonic order. Therefore, even in the critical region, this method present great results.

Finally, with the results presented in this work, it is possible to choose the best discretization methods to the harmonic detector. Depending of the harmonic order and the sampling frequencies, the choice can be made. Also, the complexity of the implementation methods needs to be take in account as well. For example, as can be seen, for low harmonic order and considerable sampling frequency, the *FB* with negative is a great option, since the results are great and present easy implementation. However, if the intention is to detect high harmonic orders with low sampling frequency, the only method which can have great performance is the *TP* and negative feedback is not necessary.

For future works, more stages of harmonic structure can be performed. In addition, experimental result can validate the methodology proposed. Also, with the experimental results, the operation time (depending of the implementation complexity of the methods) can be analyzed and take in to account for further discussion.

Referências Bibliográficas

Abbas W, Saqib MA (2007) Effect of nonlinear load distributions on total harmonic distortion in a power system. In: 2007 International Conference on Electrical Engineering, pp 1–6, DOI 10.1109/ICEE.2007.4287356

Akagi H, Kanazawa Y, Nabae A (1984) Instantaneous reactive power compensators comprising switching devices without energy storage components. IEEE Transactions on Industry Applications IA-20(3):625–630, DOI 10.1109/TIA.1984.4504460

de Andrade EG, de Oliveira HA, Ribeiro WV, de Barros RC, Pereira HA, Cupertino AF (2016) Power losses in photovoltaic inverter components due to reactive power injection. In: 2016 12th IEEE International Conference on Industry Applications (INDUSCON), pp 1–7, DOI 10.1109/INDUSCON.2016.7874587

Bonaldo JP, Paredes HKM, Pomilio JA (2013) Flexible operation of grid-tied single-phase power converter. In: 2013 Brazilian Power Electronics Conference, pp 987–992, DOI 10.1109/COBEP.2013.6785235

Bonaldo JP, Paredes HKM, Pomilio JA (2016) Control of single-phase power converters connected to low-voltage distorted power systems with variable compensation objectives. IEEE Transactions on Power Electronics 31(3):2039–2052, DOI 10.1109/TPEL.2015.2440211

Ciobotaru M, Teodorescu R, Blaabjerg F (2006a) A new single-phase pll structure based on second order generalized integrator. In: 2006 37th IEEE Power Electronics Specialists Conference, pp 1–6, DOI 10.1109/pesc.2006.1711988

Ciobotaru M, Teodorescu R, Blaabjerg F (2006b) A new single-phase pll structure based on second order generalized integrator. In: 2006 37th IEEE Power Electronics Specialists Conference, pp 1–6, DOI 10.1109/pesc.2006.1711988

Domingos RM, Xavier LS, Cupertino AF, Pereira HA (2015) Current control strategy for reactive and harmonic compensation with dynamic saturation. In: 2015 IEEE 24th International Symposium on Industrial Electronics (ISIE), pp 669–674, DOI 10.1109/ISIE.2015.7281549

Fujita H, Akagi H (1991) A practical approach to harmonic compensation in power systems-series connection of passive and active filters. IEEE Transactions on Industry Applications 27(6):1020–1025, DOI 10.1109/28.108451

He J, Li YW, Blaabjerg F, Wang X (2014) Active harmonic filtering using current-controlled, grid-connected dg units with closed-loop power control. IEEE Transactions on Power Electronics 29(2):642–653, DOI 10.1109/TPEL.2013.2255895

Lavangnananda K, Chattanachot S (2017) Study of discretization methods in classification. In: 2017 9th International Conference on Knowledge and Smart Technology (KST), pp 50–55, DOI 10.1109/KST.2017.7886082

Macii D, Barchi G, Fontanelli D (2017) Decorrelation-based harmonic distortion reduction for synchrophasor measurements. In: 2017 IEEE International Workshop on Applied Measurements for Power Systems (AMPS), pp 1–6, DOI 10.1109/AMPS.2017.8078321

Pereira HA, Domingos RM, Xavier LS, Cupertino AF, Mendes VF, Paulino JOS (2015a) Adaptive saturation for a multifunctional three-phase photovoltaic inverter. In: 17th European Conference on Power Electronics and Applications, pp 1–10

Pereira HA, Xavier LS, Cupertino AF, Mendes VF (2015b) Single-phase multifunctional inverter with dynamic saturation scheme for partial compensation of reactive power and harmonics. In: 2015 17th European Conference on Power Electronics and Applications (EPE'15 ECCE-Europe), pp 1–10, DOI 10.1109/EPE.2015.7309241

Peterson M, Singh BN, Rastgoufard P (2008) Active and passive filtering for harmonic compensation. In: 2008 40th Southeastern Symposium on System Theory (SSST), pp 188–192, DOI 10.1109/SSST.2008.4480217

Pinto JG, Pregitzer R, Monteiro LFC, Couto C, Afonso JL (2007) A combined series active filter and passive filters for harmonics, unbalances and flicker compensation. In: 2007 International Conference on Power Engineering, Energy and Electrical Drives, pp 54–59, DOI 10.1109/POWERENG.2007.4380200

REN21 (2017) Renewables 2017 global status report. REN21 Secretariat

Rodriguez FJ, Bueno E, Aredes M, Rolim LGB, Neves FAS, Cavalcanti MC (2008) Discrete-time implementation of second order generalized integrators for grid converters. In: 2008 34th Annual Conference of IEEE Industrial Electronics, pp 176–181, DOI 10.1109/IECON.2008.4757948

Rodriguez P, Luna A, Candela I, Mujal R, Teodorescu R, Blaabjerg F (2011) Multiresonant frequency-locked loop for grid synchronization of power converters under distorted grid conditions. IEEE Transactions on Industrial Electronics 58(1):127–138, DOI 10.1109/TIE.2010.2042420

Romero-Cadaval E, Spagnuolo G, Franquelo LG, Ramos-Paja CA, Suntio T, Xiao WM (2013) Grid-connected photovoltaic generation plants: Components and operation. IEEE Industrial Electronics Magazine 7(3):6–20, DOI 10.1109/MIE.2013.2264540

Sangwongwanich A, Yang Y, Blaabjerg F (2016) A cost-effective power ramp-rate control strategy for single-phase two-stage grid-connected photovoltaic systems. In: 2016 IEEE Energy Conversion Congress and Exposition (ECCE), pp 1–7, DOI 10.1109/ECCE.2016.7854671

Schmela M, Masson G (2016) Global market outlook for solar power 2016. Solar Power Europ

Song B, Xu L, Lu X (2014) A comparative study on tustin rule based discretization methods for fractional order differentiator. In: 2014 4th IEEE International Conference on Information Science and Technology, pp 515–518, DOI 10.1109/ICIST.2014.6920529

Tao W, Li J, Gu Z, Wang L (2016) Study and comparison on standard for interconnecting distributed resources with electric power systems. In: 2016 IEEE 8th International Power Electronics and Motion Control Conference (IPEMC-ECCE Asia), pp 1000–1005, DOI 10.1109/IPEMC.2016.7512423

Tummuru NR, Mishra MK, Srinivas S (2014) Multifunctional vsc controlled microgrid using instantaneous symmetrical components theory. IEEE Transactions on Sustainable Energy 5(1):313–322, DOI 10.1109/TSTE.2013.2283739

Varma RK, Das B, Axente I, Vanderheide T (2011) Optimal 24-hr utilization of a pv solar system as statcom (pv-statcom) in a distribution network. In: 2011 IEEE Power and Energy Society General Meeting, pp 1–8, DOI 10.1109/PES.2011.6039864

Xavier LS, Cupertino AF, Mendes VF, Pereira HA (2015) A novel adaptive current harmonic control strategy applied in multifunctional single-phase solar inverters. In: 2015 IEEE 13th Brazilian Power Electronics Conference and 1st Southern Power Electronics Conference (COBEP/SPEC), pp 1–6, DOI 10.1109/COBEP.2015.7420040

Xavier LS, de Jesus VMR, Cupertino AF, Mendes VF, Pereira HA (2017) Novel adaptive saturation scheme for photovoltaic inverters with ancillary service capability. In: 2017 IEEE 8th International Symposium on Power Electronics for Distributed Generation Systems (PEDG), pp 1–8, DOI 10.1109/PEDG.2017.7972556

Yepes AG, Freijedo FD, Doval-Gandoy J, Lopez, Malvar J, Fernandez-Comesaa P (2012) Correction to "effects of discretization methods on the performance of resonant controllers" [jul 10 1692-1712]. IEEE Transactions on Power Electronics 27(12):4976–4976, DOI 10.1109/TPEL.2012.2195031